

Purdue University
Purdue e-Pubs

International Compressor Engineering Conference

School of Mechanical Engineering

2008

A Design Method of the Column Envelope Meshing Pair in Single Screw Compressors

Weifeng Wu
Xi'an Jiaotong University

Quanke Feng
Xi'an Jiaotong University

Jian Xu
Xi'an Jiaotong University

Xiangling Feng
Xi'an Jiaotong University

Follow this and additional works at: <https://docs.lib.purdue.edu/icec>

Wu, Weifeng; Feng, Quanke; Xu, Jian; and Feng, Xiangling, "A Design Method of the Column Envelope Meshing Pair in Single Screw Compressors" (2008). *International Compressor Engineering Conference*. Paper 1863.
<https://docs.lib.purdue.edu/icec/1863>

This document has been made available through Purdue e-Pubs, a service of the Purdue University Libraries. Please contact epubs@purdue.edu for additional information.

Complete proceedings may be acquired in print and on CD-ROM directly from the Ray W. Herrick Laboratories at <https://engineering.purdue.edu/Herrick/Events/orderlit.html>

A Design Method of the Column Envelope Meshing Pair in Single Screw Compressors

Weifeng WU *, Quanke FENG, Jian Xu, Xiangling Feng

School of Energy & Power Engineering, Xi'an Jiaotong University,
Xi 'an, Shannxi, 710049, China
86-029-82675258, wwf.jt@163.com

ABSTRACT

A single screw compressor is an important element found in many refrigeration systems. A single screw compressor with column envelope meshing pair will have long operating life than existing single screw compressors, although it is still fail to meet industrial applications. To accelerate the industrial application of the new type compressor, a design method of column envelope meshing pair is presented in this paper, and a mathematic model of the column meshing pair is established firstly.

Keywords: single screw compressor; meshing pair; clearance; leakage; column; envelope

1. INTRODUCTION

Single screw compressors (SSCs) (Zimmern, Ganshyam and Patel, 1972) developed by Zimmern in 1960's, are widely used in refrigeration, air/gas compression and chemical engineering systems. The structure of a typical SSC is shown in Fig. 1. Essentially, a screw rotor meshes symmetrically with two star-wheels. Two star-wheels are located to double the swept volume and balance thrust (Zimmern, Ganshyam and Patel, 1972). Angular velocity ω of star-wheel and screw rotor has a relation shown as following:

$$p = \frac{\omega_b}{\omega_a} = \frac{n_a}{n_b} = \frac{11}{6}$$

Here, p is compression ratio, n is teeth number, subscript a and b indicate star-wheel and screw rotor. In most cases, $p = 11/6$ is selected.

The performance of so designed a SSC is superior to that of a single piston design (Bein, 1991) and screw compressors (ZHANG Sen, 2007). A new SSC could run with high efficiency, but its discharge capacity decreases sharply after several hundred hours of initial operation. Reason for this situation is that existing original profile of the meshing pair is straight line envelope meshing pair (SEMP). Its contact area between the star-wheel tooth flank and the screw rotor is a fixed straight line on the star-wheel tooth flank, the wear resistance is poor. Therefore Zimmern developed the column (frustum) envelope meshing pair (CEMP) (1976) to improve efficiency and operating life of SSCs. Although it is still fail to meet industrial applications for its machining method and design method.

To accelerate the industrial application of CEMP, a mathematical model of the basic rotor profile of a SSC was presented by S-C Yang (2002). And the CEMP profile was improved by David to improve its machinability (2000). However, little attention has been paid to the mathematical model of the CEMP of SSCs. This paper presents a design method of CEMP in SSCs. Coordinate systems are set up to describe the kinematic relation between the star-wheel and screw rotor, than mathematic model of the column meshing pair is established to facilitate the discussion of its design method.

2. MATHEMATICAL MODEL OF THE CEMP

CEMP was developed on the basis of the LEMP. The basic idea of this meshing pair is to replace the straight line of the original meshing pair with the column surface, and the screw groove flank (SGF) on screw rotor is consequently changed. The contacting position on the star-wheel tooth flank with the SGF changes with the revolution of the screw rotor. The varying contact position is limited in an area marked by α on the column in Fig. 2. Here the section lines of the star-wheel tooth are hidden for clarity and the other blank spaces in the figure stand for the screw groove on the screw rotor. What needs attention is that a greater diameter d and a larger zone α would lead to longer length of the varying contact arc (marked by broken line in Fig. 2), and thus better wear resistance of the meshing pair and longer operating life of SSCs. Contrarily, the wear resistance and operating life will be worse. Here, α is determined by the envelope principle, and d is limited by the interference when machining. The limited value of d can be determined according to the kinematics,

$$d < \frac{(a - R_a) p}{\sqrt{(a - R_a)^2 p^2 + R_a^2}} b \quad (1)$$

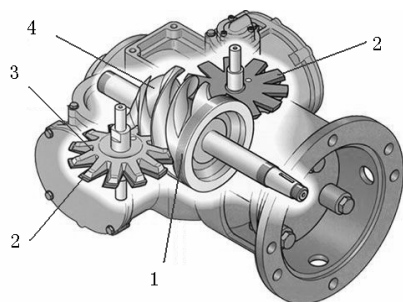


Fig. 1 Basic components of a typical single screw compressor
(1-screw rotor, 2- star-wheel and teeth, 3-support portion, 4-screw groove)

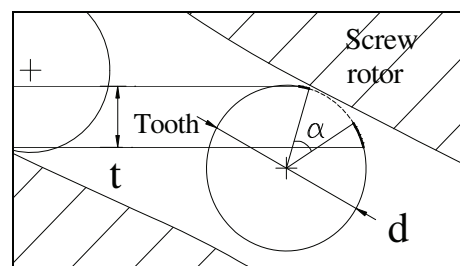


Fig. 2 CEMP

2.1 Kinetic coordinate systems

The design task of column enveloped meshing pair of SSCs is to determine the thickness t of star-wheel, the diameter d , and other geometrical parameters of the meshing pair. To mathematically describe the relationship between the star-wheel and the screw rotor, four right-handed Cartesian coordinate systems are introduced (Guangxi J. and Yan T., 1985). As indicated in Fig. 3, coordinate system Σ_1 and Σ_3 represent the stationary machine frames, the coordinate origin O_1 is coincident with the center point of the star-wheel on the center plane of the machine and its Z_1 -axis is coincident with the shaft of the star-wheel; the Z_3 -axis is coincident with the shaft of the screw rotor. Coordinate system Σ_2 assigned to the star-wheel denotes the position of the star-wheel. Coordinate system Σ_4

assigned to the screw rotor denotes the position of the screw rotor.

Here, rotational angle ϕ_a and ϕ_b have a relation shown as following:

$$\frac{\phi_b}{\phi_a} = p \tag{2}$$

Assumption that point A is on a tooth flank, the vector A in coordinate system Σ_2 can be transformed to Σ_4 by coordinate transmission:

$$\vec{A}_{\Sigma_2} = [x_2 \quad y_2 \quad z_2]' \tag{3}$$

$$\vec{A}_{\Sigma_4} = \begin{bmatrix} -x_2 \sin \phi_a \cos \phi_b - y_2 \cos \phi_a \cos \phi_b - z_2 \sin \phi_b + a \cos \phi_b \\ -x_2 \sin \phi_a \sin \phi_b - y_2 \cos \phi_a \sin \phi_b + z_2 \cos \phi_b + a \sin \phi_b \\ -x_2 \cos \phi_a + y_2 \sin \phi_a \end{bmatrix} \tag{4}$$

2.2 SGFs on the screw rotor

SGF is an envelope of tooth flank, which is a column. So the approach for solution is based on the condition of contact between the cylindrical tooth flank and SGF, namely, that the relative velocity of the surfaces at the contact points must be orthogonal to its normal vector (S.K.KANG, K.F.EHMANN and C.LIN, 1996).

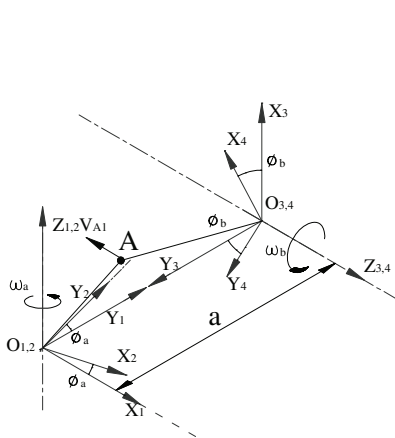


Fig. 3 Kinetic coordinate systems of CP type SSCs

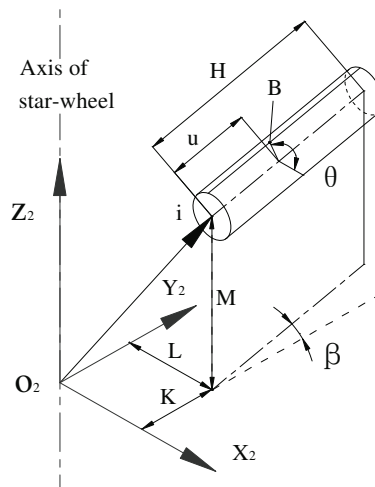


Fig. 4 The envelope column in coordinate system Σ_2

Assumption that a column which represents the tooth flank is fixed in the coordinate system Σ_2 shown in Fig. 4, and the axis of the column is normal to the Z_2 -axis. Here in Fig. 4, i - the column and a vertex of the column; B - an arbitrary external point on the column "i"; H -the height of the column; L , K , M and β describe the position of the column "i" in the coordinate system Σ_2 together; u and θ describe position of point "B" on the column "i"; the sign of β is determined by the spiral right rules as a plus sign in Fig.3. So the position of point B in Fig. 4 can be given as shown in equation (5)

$$\vec{B}_{\Sigma_2} = [x_{B2} \quad y_{B2} \quad z_{B2}]' \tag{5}$$

Here

$$\begin{cases} x_{B2} = L - u \sin \beta + \frac{d}{2} \cos \theta \cos \beta \\ y_{B2} = K + u \cos \beta + \frac{d}{2} \cos \theta \sin \beta \quad (0 \leq \theta < 2\pi, 0 \leq u \leq H) \\ z_{B2} = M + \frac{d}{2} \sin \theta \end{cases}$$

On assumption that point “B” is a contact point when the coordinate system Σ_2 turns over ϕ_a . So the normal vector of the column at point “B” and the relative in the machine frame should obey the aforementioned contact condition given as shown in equation(6):

$$\overline{v_{\Sigma_3}} \cdot \overline{n_{\Sigma_3}} = 0 \quad (6)$$

Here the subscript “ Σ_3 ” represents the variable evaluated in the coordinate system Σ_3 . For the reason of terseness and convenience, all the vectors will be evaluated in the stationary coordinate system Σ_3 . The normal vector $\overline{n_{\Sigma_3}}$ can be given as shown in equation(7):

$$\overline{n_{\Sigma_1}} = \begin{bmatrix} -\cos \theta \cos (\beta + \phi_a) \\ \sin \theta \\ -\cos \theta \sin (\beta + \phi_a) \end{bmatrix} \quad (7)$$

According to the kinematics between the star-wheel and the screw rotor, the relative velocity of point “B” is an adding of relative velocity between point “B” and coordinate system Σ_1 and relative velocity between coordinate system Σ_4 and point “B”. So relative velocity of point “B” is given as shown in equation (8)

$$\overline{v_{B3}} = \overline{v_{\Sigma_3}^I} - \overline{v_{\Sigma_3}^{II}} = \omega_a \begin{bmatrix} y_{B2} \sin \phi_a - x_{B2} \cos \phi_a - pz_{B2} \\ p(a - y_{B2} \cos \phi_a - x_{B2} \sin \phi_a) \\ y_{B2} \cos \phi_a + x_{B2} \sin \phi_a \end{bmatrix} \quad (8)$$

So the engagement between the tooth flank of the star-wheel and the SGF of the screw rotor can be simplified by substituting equation(8), equation (5) and equation (7) into equation (6) and expressed as shown in equation (9)

$$E(u, \phi_a) \cos \theta - F(u, \phi_a) \sin \theta = 0 \quad (9)$$

Here,

$$\begin{cases} E(u, \phi_a) = L \sin \beta - K \cos \beta + pM \sin (\beta + \phi_a) - u \\ F(u, \phi_a) = p [K \cos \phi_a + L \sin \phi_1 + u \cos (\beta + \phi_a) - a] \end{cases} \quad (10)$$

The angle θ can be obtained from equation (9) and equation(10):

$$\theta(u, \phi_a) = \text{arctg} \left[\frac{E(u, \phi_a)}{F(u, \phi_a)} \right] \quad (11)$$

Or

$$\theta(u, \phi_a) = \pi + \operatorname{arctg} \left[\frac{E(u, \phi_a)}{F(u, \phi_a)} \right] \quad (12)$$

Here, equation (11) is valid when the SGF engaging with the right flank of the tooth and equation (12) is valid when the SGFs engaging with the left flank of the tooth.

Finally the SGF on screw rotor can be deduced from substituting equation (5) to equation(4), and expressed as shown in equation(13):

$$\varphi(u, \phi_a, \phi_b, \theta) = \left[\chi(u, \phi_a, \phi_b, \theta) \quad \eta(u, \phi_a, \phi_b, \theta) \quad \xi(u, \phi_a, \phi_b, \theta) \right]' \quad (13)$$

Here

$$\left\{ \begin{array}{l} \chi(u, \phi_a, \phi_b, \theta) = \left(L - u \sin \beta + \frac{d}{2} \cos \theta \cos \beta \right) \cos \phi_a \sin \phi_b + \left(M + \frac{d_i}{2} \sin \theta \right) \cos \phi_b \\ \quad + a \sin \phi_b - \left(K + u \cos \beta + \frac{d}{2} \cos \theta \sin \beta \right) \sin \phi_a \sin \phi_b \\ \eta(u, \phi_a, \phi_b, \theta) = \left(L - u \sin \beta + \frac{d}{2} \cos \theta \cos \beta \right) \cos \phi_a \cos \phi_b - \left(M + \frac{d}{2} \sin \theta \right) \sin \phi_b \\ \quad + a \cos \phi_b - \left(K + u \cos \beta + \frac{d}{2} \cos \theta \sin \beta \right) \sin \phi_a \cos \phi_b \\ \xi(u, \phi_a, \phi_b, \theta) = \left(L - u \sin \beta + \frac{d}{2} \cos \theta \cos \beta \right) \sin \phi_a + \left(K + u \cos \beta + \frac{d}{2} \cos \theta \sin \beta \right) \cos \phi_a \end{array} \right.$$

Considering equation (11) and equation (2), there are only two parameters of u and ϕ_a in equation (13) independent, so equation (13) can be simplified by substituting equation (11) and equation (2) into it, so the SGF on the screw rotor can be expressed as shown in equation (14):

$$\varphi(u, \phi_a) = \varphi(u, \phi_a, \phi_b, \theta) = \left[\chi(u, \phi_a, \phi_b, \theta) \quad \eta(u, \phi_a, \phi_b, \theta) \quad \xi(u, \phi_a, \phi_b, \theta) \right]' \quad (14)$$

With the ranges of the parameters shown in equation(15):

$$\begin{aligned} 0 &\leq u \leq H \\ -\arcsin \left(\frac{a - R_b}{R_a} \right) &\leq \phi_a \leq \arcsin \left(\frac{a - R_b}{R_a} \right) \end{aligned} \quad (15)$$

2.3 The tooth flank of the star-wheel

On the other hand, the contact area on the column can obtain by substituting equation (11) or (12) into equation(5), and expressed as following:

$$\bar{C}_{\Sigma 2} = \left[\kappa(u, \phi_a) \quad \tau(u, \phi_a) \quad \sigma(u, \phi_a) \right]' \quad (16)$$

Where

$$\begin{aligned}
\kappa(u, \phi_a) &= L - u \sin \beta + \frac{d}{2} \cos[\theta(u, \phi_a)] \cos \beta \\
\tau(u, \phi_a) &= K + u \cos \beta + \frac{d}{2} \cos[\theta(u, \phi_a)] \sin \beta \quad (0 \leq u \leq H) \\
\sigma(u, \phi_a) &= M + \frac{d}{2} \sin[\theta(u, \phi_a)]
\end{aligned} \tag{17}$$

Because that there are two independent parameters in equation(16), the instantaneous contacting line equation can be given by confirming the angular parameter ϕ_a . If the value of height parameter u is given, equation (16) would describe the varying contact arc (marked by broken lines in Fig. 2) on the tooth flank.

3 A DESIGN METHOD FOR THE MESHING PAIR

One important application of the equations aforementioned is the design of the CEMP. And this design work will be after the complete appliance design of SSCs, which determines the value of the diameters of the screw rotor and the star-wheel, the length, the width of the star-wheel tooth and the centric distance between the screw rotor and the star-wheel, according to the required discharge capacity, intake and discharge pressure. So the design work of meshing pair would focus on the determination of the values of the parameters of L , K , M , H , β , d and the thickness t of the star-wheel tooth. In a general way, β is evaluated by experience, And the diameter of the column d could be evaluated as a maximum diameter of milling cutter when machining.

Take the right flank of the star-wheel tooth as an example. The vertex of the column at the root of the tooth can be determined according to envelope column diameter d . The position of the column at the tooth root section is shown in Fig. 5. At first, assumed that the pedal from the vertex to Z_2 -axis is $R_a - l$, where l is the length of the tooth. An angle parameter γ is introduced to describe the position of the column, so the value of M , L and K is shown in equation(18), (19) and(20).

$$M = -\frac{d}{2} \cos \gamma \tag{18}$$

$$L = \frac{b}{2} - \frac{d}{2} \sin \gamma \tag{19}$$

$$K = \sqrt{(R_a - l)^2 - L^2} = \sqrt{(R_a - l)^2 - \left(\frac{b}{2} - \frac{d}{2} \sin \gamma\right)^2} \tag{20}$$

Then the radian interval used as the tooth flank at the root of the tooth is shown in equation(21):

$$\frac{\pi}{2} - \arccos \frac{2M - t}{d} \leq \theta \leq \frac{\pi}{2} - \arccos \frac{2M + t}{d} \tag{21}$$

Where the value of M is bigger than the value of $t/2$ by experience. Supposition $u = 0$, and substituting equation(18), (19) and(20) in to equation (11), the engaging radian angle is obtained by equation(22):

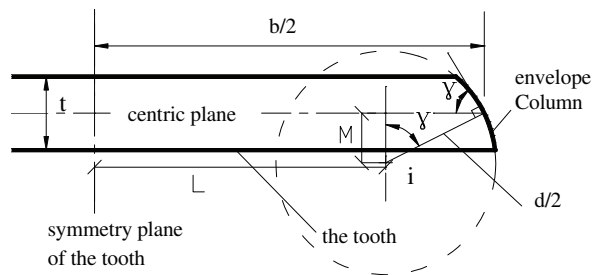


Fig. 5 Position of the column at the tooth root

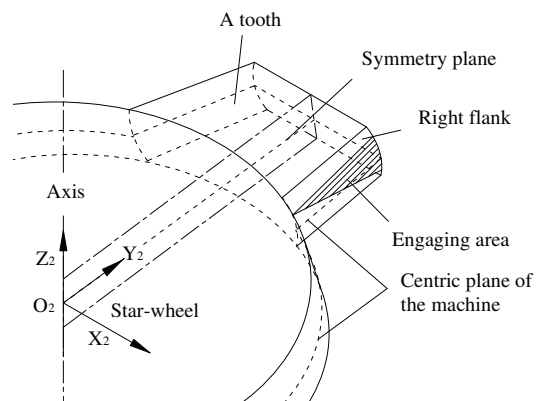


Fig. 6 Tooth profile of CEMP

$$\theta(\gamma, \phi_a) = \arctg \left[\frac{E(\gamma, \phi_a)|_{u=0}}{F(\gamma, \phi_a)|_{u=0}} \right] \quad (22)$$

Here, according to the engagement between the star-wheel and the screw rotor, the radian interval of ϕ_a is shown in equation (23)

$$-\arcsin\left(\frac{a-R_b}{R_a}\right) \leq \phi_a \leq \arcsin\left(\frac{a-R_b}{R_a}\right) \quad (23)$$

The length of the column is

$$H = \frac{l}{\cos \beta} \quad (24)$$

Now, let $\gamma = \gamma_0$, and substituting equation(18), (19), (20) and equation (24) into equation (11), and make sure the functional value of $\theta(u, \phi_a)$ belongs to the interval given by equation (21). If the functional value is outside the interval given by equation(21), another value of γ_0 should be found and upper steps should be carried out again till the functional value of $\theta(u, \phi_a)$ meets the demands. A diagrammatic sketch of the result is shown in Fig. 6.

In most cases, there are many values of γ_0 meet the demands aforementioned. Further improvement can be obtained from the lubricating and the balancing of gas forces on the star-wheel tooth, which are not discussed here.

Then, the other important application is the machining method for the CEMP on the screw rotor. The mathematical model of SSCs can be obtained by the equation (14) before machining. So, a simulation and analysis of machining with CAD programs is available, which will enhance the efficiency and precision of machining.

4 CONCLUSIONS

The column meshing pair will have good wearing-resistant performance for the reason of wide contacting area on the tooth flank between the meshing pair. Milling availability is another advantage of the CEMP. The machining method should obey the column envelope principles described by equations aforementioned strictly.

Mathematical model of CEMP is proposed based on kinematics and geometry. And design method of the meshing pair is given after the mathematical model. To modify the design method, suitable value of γ_0 can be chosen further by lubrication and leakage conditions in the compressor.

NOMENCLATURE

p	Compressor ratio	L, K, M	coordinates values of the point "i"
ω	Angular velocity	H	Length of the enveloping column
d	Diameter	\vec{n}	Surface normal
a	Centric distance of the meshing pair	\vec{v}	Velocity vector
R	Radius	β	Angle between Y2-axis and envelope column axis
α	Enveloping angle	t	Thickness of the star-wheel tooth
ϕ	Rotational angle	b	Tooth width of the star-wheel

REFERENCE

- Bein, T. W. 1991, High pressure single screw compressors. US Pat. 4981424.
- Bernard Z., Dr.Ganshyam, C.Patel, 1972, Design and Operating Characteristics of the Zimmern Single Screw Compressor, Compressor Technology Conference, Purdue: 96-99.
- Bernard Z., 1976, Rotary injection worm and worm wheel with specific tooth shape, US Pat.3932077.
- Bernard Z., Method and a screw machine for processing fluid under high pressures with liquid injection between a sealing portion and a support portion of the gate rotor. 1990, US Pat. 4900239.
- Boblitt, W. W. Method for cutting complex tooth profiles in a cylindrical, single-screw gate-rotor. 1987, US Pat. 4710076.
- David J., 2000, Method for manufacturing fluid compression/compressor rotor. US Pat. 6122824.
- Guangxi J., Yan T., 1985, Resent advances in the profile study of the engagement pair of a single-screw compressor, J. Xi'an Jiaotong University, 19(6):1-9.
- S-C Y., 2002, A mathematical model of the rotor profile of the single screw compressor, Proc. Instn. Mech. Engrs. Part C: J. Mechanical Engineering Science, 216:343-351.
- S.K.KANG, K.F.EHMANN, C.LIN, 1996, A cad approach to helical groove machining-I. Mathematical model and model solution. Int. J. Mach. Tools Manufact. 36(1):141-153.
- Liu ZM, Hou DH, Wang XC, Zhang XZ, Computer aided analysis and manufacture for engagement pair of single screw compressor, 5th International Conference on Progress of Machining Technology (ICPMT 2000), 818-823.
- Bernard Z., Single screw compressor with liquid lock preventing slides. US Pat. 6106241, 2000.
- Wu ZY, Tao GL, A mathematical model of movable component in single screw compressor, 2005, Proceedings of the sixth international conference on fluid power transmission and control, 276-279.
- Shyue-Cheng Yang, Profile generation and analysis for a pp-type single-screw compressor, 2006, International Journal of Advanced Manufacturing Technology, 30(9-10):789-96.
- Wu Weifeng, Feng Quanke, Xu Jian, 2007, Principle of Multi-column Envelope Couple of Single Screw Compressor, Journal of xi'an Jiao tong university, 41(11):1271-1274.
- ZHANG Sen, 2007, The Comparision of Twin And Single Screw Refrigerating Compressor, Low Temperature and Specialty Gases, 25(03):1:4.